2026 International Conference on Computing Theory and Wireless Communications (ICCTWC)
Ichalkaranji, India. April 01-02, 2026

Dung Beetle Optimized LSTM Classifier for the Diagnosis of White Blood Cells

S.Vijayaselvarani
Department of Computer Science and Business Systems
Vel Tech Multi Tech Dr.Rangarajan Dr.Sakunthala Engineering College,
Avadi - Chennai – 600062, India.
vijayaselvarani.s@gmail.com

Deepa Manokaran
Department of Management Studies
Saveetha Engineering College,
Thandalam, Chennai, India.
deepam@saveetha.ac.in

Sathishkumar S
Department of Computer Science and Engineering
Kangeyam Institute of Technology,
Kangeyam, Tiruppur, 638108, India.
sathismecse@gmail.com

Enoch Raja DG
Department of Computer Science and Engineering
Vels Institute of Science, Technology & Advanced Studies,
Vels University,
Pallavaram, Chennai -600117, India.
enochrajadr@gmail.com

Dhivyabharathi D
Department of Computer Science and Engineering
Dhanalakshmi Srinivasan College of Engineering,
Coimbatore, India.
diyadvs@gmail.com

Jinsha Lawrence
Department of Computer Science and Engineering
Faculty of Engineering,
Karpagam Academy of Higher Education (Deemed to be University),
Coimbatore, India.
jinshalarence@gmail.com

***Abstract*— This paper proposes a diagnosis of WBCs using Dung Beetle-Optimized (DBO) Long Short-Term Memory (LSTM) classifier. An image is first pre-processed using an Iterative Mean Filter (IMF) to minimize noise in the image. The best threshold value to distinguish the foreground from background is automatically determined using the Otsu's Thresholding (OTUS) method of picture thresholding. After that, the feature extraction method of Histogram of Oriented Gradients (HOG) is employed to extract essential shape and texture information from images of blood samples. LSTM is utilized to classify different types of white blood cells with the highest accuracy or detect abnormalities. The DBO algorithm is utilized to fine-tune the learning rates, the number of hidden units, and other relevant parameters of the LSTM. The simulation is implemented in Python Software, and it achieved the highest accuracy of 99%, precision of 99%, and recall of 98% in comparison to traditional optimization techniques.**

Keywords*— *White Blood Cells, Iterative Mean Filter, Feature Extraction, Dung Beetle-Optimization.

I. Introduction

The World Health Organization (WHO) plays a key role in the global health landscape, including the regulation and management of blood safety, blood transfusions, and blood-related diseases. The WHO's efforts are crucial for ensuring the safety of blood for transfusions, improving access to safe blood for patients in need, and addressing various blood-related health issues worldwide [1]. The WHO promotes blood safety to prevent the transmission of infectious diseases through transfusions and to ensure that blood and blood products are available for medical procedures when necessary. The WHO is also involved in the fight against blood borne diseases that is transmitted through contaminated blood or unsafe transfusions. Red Blood Cells (RBCs), platelets, and WBCs make up the majority of blood [2-3]. WBCs in blood are essential for both detecting various illnesses and preventing infections. A significant indicator for the clinical diagnosis of several illnesses is the WBC count. The replication of faulty WBCs causes Leukemia, one of the worst forms of blood cancer. So, analyze and check the count of WBC, and if there is any difference, early medical treatment is essential. To overcome these limitations, computer-assisted techniques are required. Preprocessing is the first step in medical image processing. This procedure makes use of a variety of filters. One of the filters is a Gaussian filter, which uses a Gaussian distribution to average the nearby values in order to smooth the picture or signal [4-5]. Because it averages the nearby numbers, its boundaries are obscured. Its sole goal is to eliminate fuzzy images, other noises are not identified during this procedure. It is necessary since an efficient filter is used. Furthermore, as it does not retain edges as well as the median filter, it does so better than other uniform filters. To get over these issues, an effective IMF is employed in this work [6]. The next phase is the segmentation procedure. Adaptive thresholding, clustering methods, and edge-based and region-based segmentation are all employed in previous attempts. These methods are time-consuming and computationally intensive. Real-time processing becomes difficult when dealing with high-resolution photos or films due to the increase in the computing cost. As a result, one of the best OTSU segmentation techniques is used in this instance. For more intricate image processing, it serves as a pre-treatment step. Therefore, other methods are more suitable for more complicated images or situations requiring exact segmentation [7-8]. The next step in image processing is feature extraction, which transforms unprocessed data into a collection of valuable and significant characteristics or attributes. These characteristics are employed to categorize data, identify trends, or carry out additional analysis. In the context of images, feature extraction seeks to preserve important information while representing pertinent aspects of the image in a lower-dimensional format that is simpler to analyze. In this manner, the features are precisely extracted using the HOG approach. It is also made to record shape information, which is very helpful for identifying images with distinct borders. WBC image categorization faced with difficulties. In order to quickly identify the WBC, many classification methods from Machine Learning (ML) and DL are applied [9-10]. There are several ML algorithms used, most of which focus on categorizing imaging of WBCs. The ML approaches including RF, DT, and SVM. Inaccurate forecasts and misdirected insights result from this method's time delay and low-quality data. Additionally, ML has various disadvantages [11-12]. Common neural network types in DL models, such as ANN, CNN, and GNN, show promising outcomes when working with graph or network data. However, when compared to sparse or unbalanced training data, these continue to perform poorly, and they are also accessible to challenges [13–15]. During training, DL models are optimized using the DBO system.

Optimizing classification is crucial for guaranteeing the efficacy, efficiency, and dependability of classification models, particularly in complex or high-risk circumstances. Therefore, this work employs an LSTM with DBO. Consequently, the following are the following contributions are achieved:

- To enhance quality of blood cell images and preserve the important edges and structures while reducing noise, employ a median filter.
- To address variations in image intensity that occur due to differences in staining or lighting conditions and isolate different types of white blood cells, an OTSU segmentation is used.
- To extract essential shape and texture information from images of blood samples using the HOG technique.
- To identify abnormalities and detect atypical white blood cell features with high accuracy by using an LSTM-based model.
- To optimize and boost performance of LSTM model, the DBO technique is used.

II. Proposed Methodology

LSTM with DBO Algorithm is proposed in this work for diagnosis of WBCs. Fig. 1 shows processing block diagram.

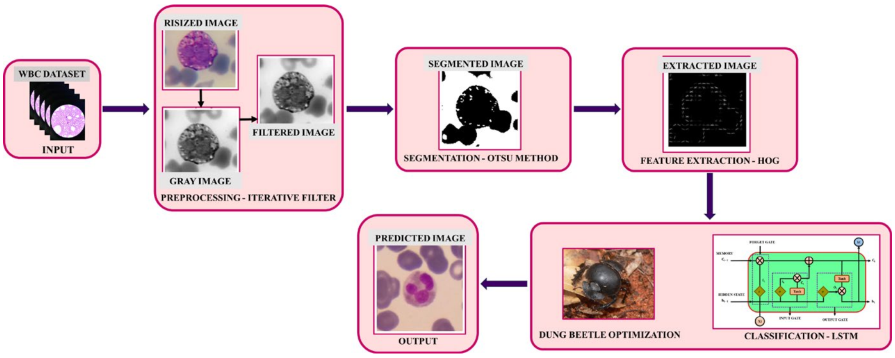

Fig. 1. Block Diagram for the Proposed Work

The initial stage of preprocessing allows an analysis of the input image by using the IMF, which works to remove noise and enhance the visibility of blurred images. Otus handles the segmentation step for this modulus after preprocessing. This image segmentation technique classifies pixels based on their intensity values. For the segmented image, the following feature extraction process. The HOG technique extracts the features for image detection and recognition quickly and accurately. Then, the DL classifier technique is allowable. Also, the LSTM classification provides excellent specificity and sensitivity for classifying images. Additionally, for the classification, the DBO is used to efficiently optimize a number of parameter values, and it improves the detection and classification. The final step is producing the output image.

A. *Preprocessing – Iterative Mean Filter*

The IMF is a technique used to reduce noise from images, particularly in medical image processing. When applied to WBC images, it helps smooth out image noise, enhancing the clarity and quality of cell boundaries and structures for better analysis. First and foremost, IMF makes use of Mean Filter's (MF's) benefit by employing a 3 x 3 window. Next, instead of employing the median, combine this benefit with a window's limited mean. In this manner, a new gray value for the central pixel is evaluated with more accuracy. IMF, like MF, is ineffectual at high noise densities because it only takes into account a fixed-size window. As a result, it is employed in conjunction with an iterative process. All noisy pixels are processed thanks to the iterative process. The `1-distance provides the basis for the iterative procedure's stop condition. In each iteration, the image becomes progressively smoother. The iterative process helps in enhancing the edge of the cells and structures by reducing pixel noise in the image.

B. *Segmentation – OSTU Method*

The OTSU approach is uses the largest inter-class variance between the target picture and the surroundings as the threshold selection criterion. The greatest between-class variance technique is likewise an alias of the OTSU method, according to its underlying idea. Based on its grayscale properties, it separates the image into foreground and background. The biggest difference between the two sections occurs when the optimal threshold is chosen. The most widely used measure standard in the OTSU method is the greatest inter-class variance. The greater the variance number, the more the two graph portions deviate from one other, as variation is a key sign of a uniform gray distribution. Incorrectly dividing some targets into backgrounds or dividing some backgrounds into targets reduces the difference between the two halves.

If an image's grayscale and the number of pixels with grayscale k is n_k, then image's total number of pixels N is,

$$N = \sum_{k=0}^{L-1} n_k = n_0 + n_1 + \cdots + n_{L-1} \tag{1}$$

The gray level k's occurrence is,

$$p_k = \frac{n_k}{N} = \frac{n_k}{\sum_{k=0}^{L-1} n_k} \tag{2}$$

Among them,

$$u(t) = \sum_{i=0}^{L-1} i p_i \tag{3}$$

The inter-class variance is defined as,

$$\sigma_w^2 = w_0\sigma_0^2 + w_1\sigma_1^2 \tag{4}$$

Then the inter-class variance is,

$$\sigma_B^2 = w_0(u_0 + u_T)^2 + w_1(u_1 + u_T)^2 \tag{5}$$

The population's inter-class variance is,

$$\sigma_T^2 = \sigma_B^2 + \sigma_w^2 \tag{6}$$

σ_B^2 represents the statistical features based on the first order, while σ_w^2 represents the statistical characteristics based on the second order. Since σ_w^2 and σ_B^2 depend on the threshold value t, while σ_T^2 is independent of t, it is easiest to select the criterion. This criterion is used to regulate optimal threshold value t. After the segmentation stage, the feature extraction is useful to extract features for classification easily.

C. Feature Extraction – HOG

HOG remains a widely used feature extraction method in vision-based systems, particularly for tasks involving the detection of images based on their shape and structural properties. HOG captures the distribution of edge directions, making it particularly useful for tasks like human detection. Within each cell, a histogram is created that accumulates the gradient magnitudes for each orientation bin. This histogram reflects the distribution of edge directions within the cell. By normalizing the gradient histograms, HOG features are less sensitive to variations in lighting conditions and contrast. Fig. 2 displays the function of HOG feature extraction.

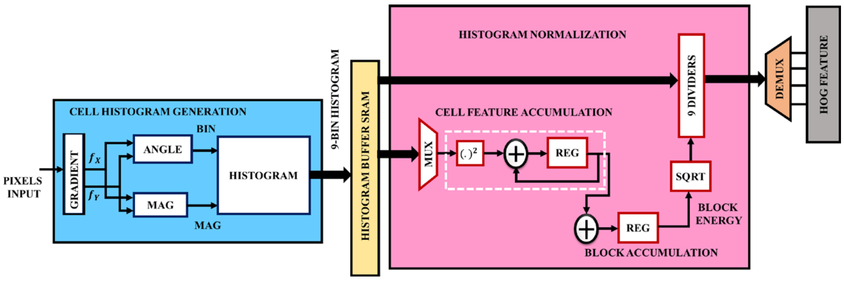

Fig. 2. Feature extraction of HOG

The proposed approach employed a greater number of histogram bins on various image regions in order to extract HOG characteristics. (7) and (8) are used to determine the gradient for each pixel in the image.

$$d_x = I(x + 1, y) - I(x, y) \tag{7}$$

$$d_y = I(x, 1 + y) - I(x, y) \tag{8}$$

After that, the gradient orientation, θ , is obtained employing (9).

$$\theta(x, y) = \tan^{-1}\frac{d_y}{d_x} \tag{9}$$

d_x and d_y denote the horizontal and vertical slopes respectively. $I(x, y)$ refers to value of a pixel (x, y) within the image.

D. Classification - LSTM

LSTM networks, a type of RNN, have proven effective in handling sequence-based data and learning long-term dependencies in data. The extracted features are passed to an LSTM, which learns the relationships and dependencies between different regions of the image or between sequential frames of image data. By combining nature-inspired optimization methods like DBO with LSTM networks, it creates an optimized model for WBC classification, but can still perform similarly to LSTM in many tasks is represented in Fig. 3.

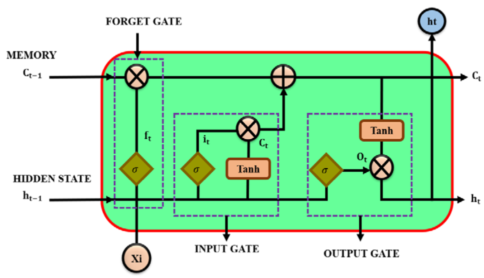

Fig. 3. Architecture of LSTM

a) Cell State (C_t):

$$C_t = tanh(W_C.[h_{t-1}, x_t] + b_C) \tag{10}$$

The "memory" of the LSTM unit, which carries information across time steps.

b) Hidden State (h_t):

$$h_t = o_t.tanh(C_t) \tag{11}$$

This output, which includes the learnt data needed for prediction, comes from the LSTM unit at a certain time step.

c) Forget Gate (f_t):

$$f_t = \sigma(W_f.[h_{t-1}, x_t] + b_f) \tag{12}$$

Which data from the prior cell state are deleted is determined by this gate.

d) Input Gate (i_t)

$$i_t = \sigma(W_i.[h_{t-1}, x_t] + b_i) \tag{13}$$

What additional data gets introduced to the cell state is decided by this gate.

e) Output Gate (o_t)

$$o_t = \sigma(W_o.[h_{t-1}, x_t] + b_o) \tag{14}$$

The portion of the cell state that are produced at the current time step is determined by this gate.

E. Dung Beetle Optimization

This approach uses to fine-tune the LSTM model parameters for better classification accuracy, especially when using complex datasets like time-series data or large-scale imaging data. The DBO algorithm successfully optimizes the hyperparameters of the LSTM model, enhancing its capacity to classify WBCs accurately. By simulating the foraging behavior of dung beetles, DBO efficiently navigates the complex search space of possible hyperparameter values, leading to an optimal set that improves the LSTM's performance.

The following is the definition of the formula for updating the position:

$$X_i(t+1) = X_i(t) + \tan(\theta) * |X_i(t) - X_i(t+1)| \quad (15)$$

The present position $X_i(t)$ and the previous position data $X_i(t-1)$ are seen to be strongly associated with position update.

The brood ball's location adjusted in accordance with the spawning area's continuous updates.

$$B_i(t+1) = b_1 \times (B_i(t) - Lb^*) + b_2 \times (B_i(t) - Ub^*) \quad (16)$$

The toddler dung location is updated:

$$X_i(t+1) = C_1 \times (X_i(t) - Lb^b) + C_2 \times (X_i(t) - Ub^b) \quad (17)$$

Whereas b^b represents a random vector, C_1 and C_2 represent random numbers.

Since the position data of thief dung beetle, it takes dung balls, is updated accordingly,

$$X_i(t+1) = X^b \times s \times g \times (|X_i(t) - X^*| + |X_i(t) - X^b|) \quad (18)$$

Wherever g denotes a random vector, S is a constant value.

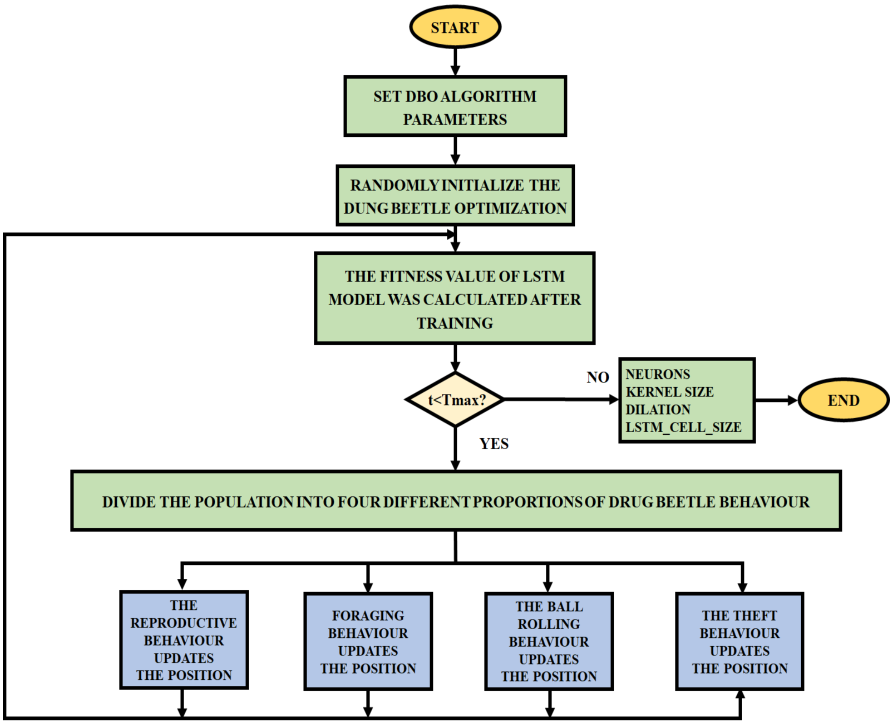

Fig. 4. Flowchart of the DBO Algorithm

Figure 4 shows the classification with DBO optimization improve the system's overall effectiveness and performance. With rise of AI, ML, and nature-inspired optimization algorithms like DBO, the accuracy and efficiency of WBC diagnosis is significantly improved, helping healthcare professionals make quicker and more reliable decisions.

III. Results and Discussion

This paper proposes the optimization and DL classification to identify WBCs. Additionally, this paper is carried out using a Python software tool for WBCs diagnosis, and the outcomes are presented below.

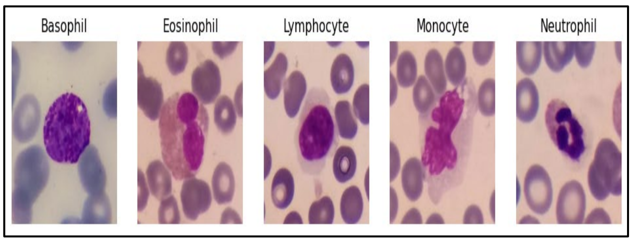

Fig. 5. Input Image

Figure 5 displays the 5 types of input WBC image datasets. These categories illustrate the diagnosis of WBC disorders. An image is selected to serve as the input.

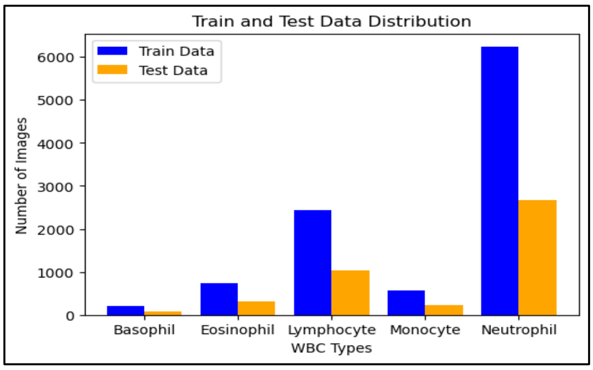

Fig. 6. Distributions of dataset

The distribution of the test and train datasets is displayed in Fig. 6. It indicates that the neutrophils in dataset much exceeds number of cell types.

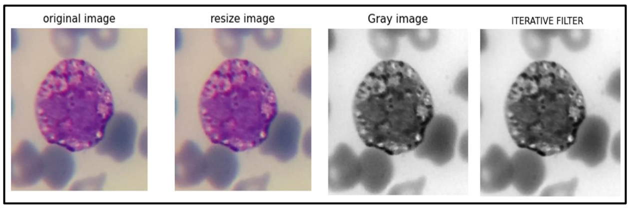

Fig. 7. Preprocessed Image by Using IMF

Figure 7 shows an image that has been preprocessed using an IMF. Pre-processing involves resizing the original image and converting the colour image to grayscale. The supplied gray image is also subjected to an iterative filter, and the output of the IMF is obtained.

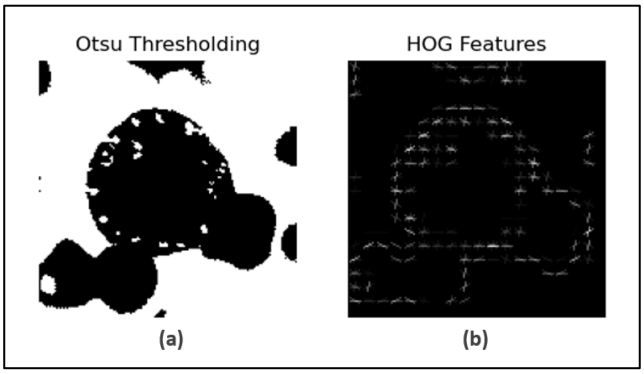

Fig. 8. Segmented and Feature Extraction Images

Figure 8 illustrates the (a) segmented image and (b) feature extraction image in various input image. In the Figure, (a) segmented images are used in the OTUS thresholding method to segment the region of the dataset. Following that, Figure (b) the HOG methodology offers an effective technique for extracting the features.

TABLE I. Classification Report

Classification	
Accuracy	99%
Precision %	99%
Recall%	98%
F1- Score%	97%

Table I shows with the WBC classification, it indicates the 99% predicted and actual accuracy, 99% precision, 98% recall, and 97% F1 score.

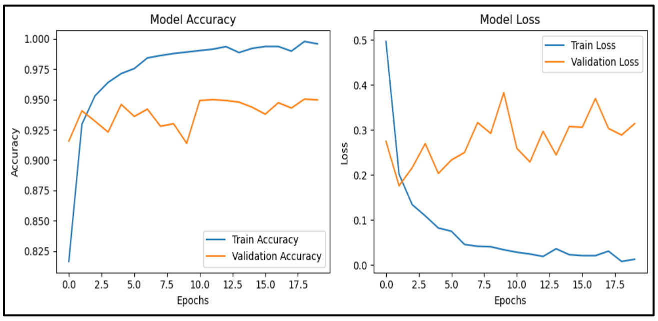

Fig. 9. Model Accuracy and Model Loss

Figure 9 provides instances of the model. Accuracy curves and training and validation losses are clearly seen in the Fig. 9, respectively.

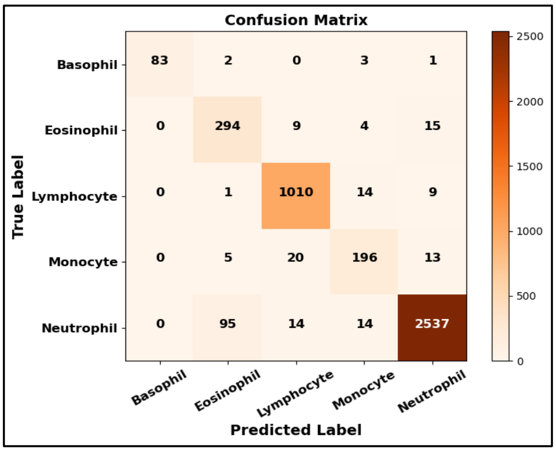

Fig. 10. Confusion Matrix Graph

The predicted and true labels are shown in Fig. 10, where the WBC classification neutrophil is at the top of the matrix.

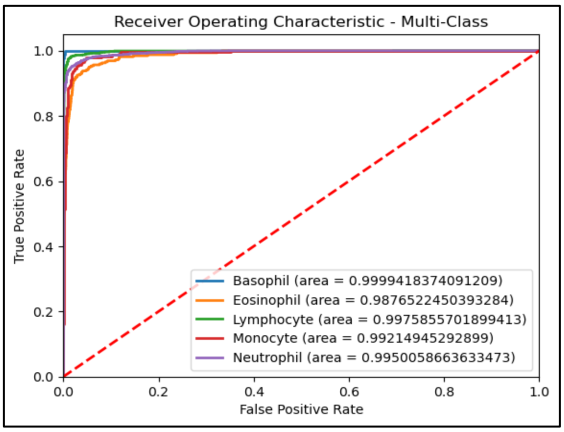

Fig. 11. ROC Curve

The DBO-LSTM classification is illustrated in Fig. 11. The DBO-LSTM achieves 99% classification accuracy.

TABLE II. Comparison performance of various classifications

Methods	Accuracy %	Precision %	Recall %	F1-Score%
VGG [14]	94.4	90.14	92.17	96.14
CNN [13]	97.51	96.41	93.3	97.75
Efficient Net B3-Adam Optimizer [10]	98.3	97.65	98.12	98.22
Proposed DBO - LSTM	99	99	98	97

Table II represents the performance of comparative analysis of previous classifications and the proposed classification. Accuracy, precision, recall, and F1 score for the VGG [14] classification are 94.4%, 90.14%, and 92.17%, respectively, in the table. 97.51% accuracy, 96.41% precision, 93.3% recall, and 97.75% F1 score are attained with the CNN [13] categorization. The Efficient Net B3-Adam optimizer [10] is attained with an accuracy of 98.3%, precision of 97.65%, recall of 98.12%, and F1 score of 98.22%. The proposed DBO-LSTM is accuracy of 99%, precision of 99%, recall of 98%, and F1-score of 97% are achieved.

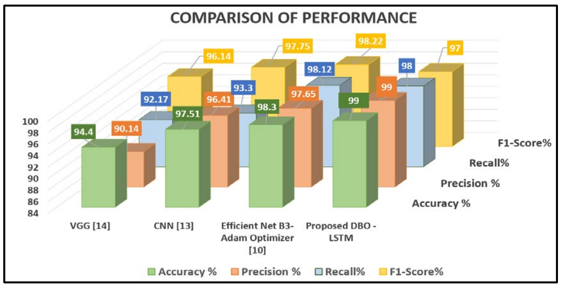

Fig. 12. Comparison of Performance

Figure 12 displays the performance of the proposed LSTM classification along with a comparative graph of several classes. Alternative classifications with accuracy and loss values, such as VGG [14], CNN [13] and Efficient Net B3- Adam Optimizer [10] have been observed. Finally, the proposed approach demonstrated the highest validation accuracy compared to others.

IV. Conclusion

This paper proposes the DBO-LSTM classifier offered for the automated diagnosis of WBC disorders. Otsu's method is highly useful for segmenting WBCs from the background of blood smear images. The DBO optimization algorithm helped in tuning the hyper parameters of the LSTM network, thus improving to classify various types of WBCs. Further, it achieves the accuracy and performance of WBC classification tasks. Overall, this work demonstrates higher accuracy of 99%, precision of 99%, and recall of 98% in diagnosing WBC types and detecting abnormalities. The optimization process ensures that model is better equipped to handle variations in WBC features, which are critical for early disease detection.

References

[1] H. Shen, "Yongliang Ouyang, Liang Zhang, Jing Li, and Shige Wang. "Blood cell membrane-coated nanomaterials as a versatile biomimetic nanoplatform for antitumor applications," Nanomaterials, vol. 14, no. 21, pp. 1757, 2024.

[2] D. Wang, "White blood cell membrane-coated nanoparticles: recent development and medical applications," Advanced Healthcare Materials, vol. 11, no. 7, pp. 2101349.Z, 2022.

[3] Z. Wang, "Automatic Classification of White Blood Cells Using a Semi-Supervised Convolutional Neural Network," in IEEE Access, vol. 12, pp. 44972–44983, 2024.

[4] D. Hussain, "Exploiting the Multiscale Information Fusion Capabilities for Aiding the Leukemia Diagnosis Through White Blood Cells Segmentation," in IEEE Access, vol. 10, pp. 48747–48760, 2022.

[5] S.S. Mahmoud, "Efficient Malaria Parasite Detection From Diverse Images of Thick Blood Smears for Cross-Regional Model Accuracy," in IEEE Open Journal of Engineering in Medicine and Biology, vol. 4, pp. 226–233, 2023.

[6] E. George, "Detection of Acute Lymphoblastic Leukemia Using a Novel Bone Marrow Image Segmentation," in Tsinghua Science and Technology, vol. 30, no. 2, pp. 610-623, April 2025.

[7] A. Munshi, "Prediction of Anemia from Multi-Data Attribute Co-Existence," in IEEE Access, vol. 12, pp. 182923-182942, 2024.

[8] Z. Lu, "White Blood Cells Image Classification Based on Radiomics and Deep Learning," in IEEE Access, vol. 10, pp. 124036-124052, 2022.

[9] D. Hanbay, "Improving Cell Image Segmentation by Using Isotropic Undecimated Wavelet Transform," in IEEE Access, vol. 12, pp. 159902-159912, 2024.

[10] J. Chen, "A Miniaturized and Intelligent Lensless Holographic Imaging System With Auto-Focusing and Deep Learning-Based Object Detection for Label-Free Cell Classification," in IEEE Photonics Journal, vol. 16, no. 3, pp. 1-8, June 2024.

[11] K. Kim, "Lightweight and Efficient YOLOv8 With Residual Attention Mechanism for Precise Leukemia Detection and Classification," in IEEE Access, vol. 12, pp. 159395-159413, 2024.

[12] T. C. Akinci, "Assessment of Hematological Predictors via Explainable Artificial Intelligence in the Prediction of Acute Myocardial Infarction," in IEEE Access, vol. 11, pp. 108591-108602, 2023.

[13] Y. Liu, "Improved generalization of white blood cell classification by learnable illumination intensity invariant layer," IEEE Signal Process. Lett., vol. 31, pp. 176–180, 2024.

[14] M. Zhang, "Blood cell detection method based on improved YOLOv5," IEEE Access, vol. 11, pp. 67987–67995, 2023.

[15] H. Alhussian, "A comprehensive systematic review of Yolo for medical object detection (2018 to 2023)," IEEE Access, vol. 12, pp. 57815–57836, 2024.